



OPEN

Heatwaves during low tide are critical for the physiological performance of intertidal macroalgae under global warming scenarios

Marta Román^{1,2}✉, Salvador Román^{1,2}, Elsa Vázquez^{1,2}, Jesús Troncoso^{1,2} & Celia Olabarria^{1,2}

The abundance and distribution of intertidal canopy-forming macroalgae are threatened by the increase in sea surface temperature and in the frequency and intensity of heatwaves caused by global warming. This study evaluated the physiological response of predominant intertidal macroalgae in the NW Iberian Peninsula (*Bifurcaria bifurcata*, *Cystoseira tamariscifolia* and *Codium tomentosum*) to increased seawater temperature during immersion and increased air temperatures during consecutive emersion cycles. We combined field mensuration and laboratory experiments in which we measured mortality, growth, maximum quantum yield and C:N content of the macroalgae. Air temperature was a critical factor in determining physiological responses and survivorship of all species, whereas high seawater temperature had sublethal effects. *Cystoseira tamariscifolia* suffered the greatest decreases in F_v/F_m , growth and the highest mortality under higher air temperatures, whereas *C. tomentosum* was the most resistant and resilient species. Two consecutive cycles of emersion under atmospheric heatwaves caused cumulative stress in all three macroalgae, affecting the physiological performance and increasing the mortality. The potential expansion of the warm-temperate species *B. bifurcata*, *C. tamariscifolia* and *C. tomentosum* in the NW Iberian Peninsula in response to increasing seawater temperature may be affected by the impact of increased air temperature, especially in a region where the incidence of atmospheric heatwaves is expected to increase.

Sublittoral and intertidal canopy-forming macroalgae form the basis of coastal trophic webs and support economic activities such as fisheries and tourism in many coastal regions^{1,2}. In the present context of global warming, macroalgae are potentially important contributors to carbon sequestration³, although they are also threatened by the expected increases in seawater temperature⁴ and air temperature^{5,6}. Gaining an understanding of the vulnerability of macroalgae to global warming is therefore of great ecological and socio-economic concern.

The most likely situation under a baseline scenario for future climate change (i.e. a scenario in which no efforts have been made to reduce greenhouse gas emissions) will be a balance between representative concentration pathways (RCP) 6.0 and 8.5⁷. Under this scenario, it has been estimated that the global temperature is likely to increase by between 2.25 and 3.7 °C by 2081–2100, relative to the 1986–2005 values. Moreover, climate change will probably lead to increased frequency, intensity and duration of heatwaves^{7–9}.

Temperature strongly influences the survival, recruitment, growth and reproduction of seaweeds¹⁰. Previous studies have examined how the physiology of intertidal fucoids and kelps is affected by increases in seawater temperature^{11,12} or increases in air temperature^{13–15}. The effect of acute thermal stress events on macroalgae is of high importance, as physiological traits of intertidal macroalgae, such as growth, nutrient uptake and photosynthetic performance, are negatively affected by marine heatwaves^{16–19}. Direct exposure of the fronds to intense sunlight, increased air temperature due to atmospheric heatwaves and desiccation during emersion at low tide are also detrimental to the physiological performance of macroalgae^{6,20,21}, decreasing photosynthetic activity and leading to oxidative stress^{22,23}. In temperate zones, aerial thermal stress generally peaks in summer, on clear calm

¹Departamento de Ecología E Biología Animal. Facultade de Ciencias Do Mar, Universidade de Vigo, Campus Lagoas-Marcosende, s/n, 36310 Vigo, Pontevedra, Spain. ²CIM. Grupo de Ecología Costeira, Edificio CC Experimentais, Universidade de Vigo, Campus de Vigo, As Lagoas, Marcosende, 36310 Vigo, Spain. ✉email: marroman@uvigo.es

days when low tide occurs in mid-afternoon²⁴. If such conditions persist during few consecutive days, physiological performance of macroalgae may be negatively affected as the conditions will lead to harsh thermal and desiccation stresses^{15,20}. Thus, for example, the kelp *Laminaria digitata* (Hudson) J. V. Lamouroux showed reduced resilience after repeated exposure to atmospheric heatwaves on emersion^{25,26}. These two types of warming are, therefore, important drivers in the global distribution of intertidal canopy-forming macroalgae, leading to species decline and range shifts^{27–30} with further consequences on the structure and functioning of communities and entire ecosystems^{16,31–33}. This is the case of the fucoid *Fucus serratus* Linnaeus, which has undergone a westward shift in distribution in northern Spain in the last few decades, so that it is now almost entirely limited to scattered populations³⁴ as a consequence of the increased seawater and air temperatures^{20,35}. Such changes have altered the structure of benthic invertebrate assemblages and shortened the length of the food chain³⁶.

The combination of atmospheric and marine heatwaves has been reported to cause high mortality and abundance losses of *Durvillaea* spp. along the New Zealand coast³⁷. However, there are few laboratory experiments that have studied the combined effects of both stressors (see²⁰). Physical stressors may act additively, synergistically or antagonistically³⁸. Synergistic interactions between increased air and seawater temperatures may have greater impacts and unexpected negative responses as the response will be greater than that predicted from the effect of each individual stressor³⁸. In the fucoid *F. serratus*, air and seawater temperatures act additively²⁰, which suggests that these stressors may exert some general effects on macroalgae. Consecutive periods of exposure at low tide within a single spring tidal cycle can also affect the physiological response of some species^{21,25,26}. The effect of different temperatures during consecutive emersion cycles is yet unknown and it should therefore be taken into account by replicating low tide exposure experienced in the field²⁵. Further research is required to address the cumulative effects of thermal stress on the physiology of intertidal macroalgae, the additive effects of stressors and the potential consequences for the future distribution of these organisms.

In the NW Iberian Peninsula, the air temperature has increased by 0.5 °C·decade⁻¹ since 1974 and the coastal surface seawater temperature has increased by 0.15 °C·decade⁻¹ since 1985³⁹. These changes are expected to intensify in the future^{40,41}; for example, the seawater temperature in the Iberian upwelling is expected to increase by 2.4 °C in the period 2070–2100⁴¹. Distributional shifts due to increasing seawater temperature have already occurred along the northern Iberian Peninsula, with a clear northward expansion of warm-water species over the last decade^{30,42}, together with a decline in some habitat-forming species such as kelps and fucoids^{27,43,44}. Increased seawater temperature has led to changes in the distribution of populations of the intertidal fucoids (Ochrophyta) *Bifurcaria bifurcata* R. Ross and *Cystoseira tamariscifolia* Hudson and of the green macroalga *Codium tomentosum* Stackhouse. Populations of these species currently co-occur, covering large areas of the rocky intertidal shore on emergent rock or in rock pools along the northwestern Iberian Peninsula^{45,46}. The abundance and distribution of both *B. bifurcata* and *C. tamariscifolia* have increased in a westward direction on the northern coast of Spain, and the observed patterns have been linked to recent increases in sea surface temperature^{28,44,47}. Predictive models for global warming scenarios indicate that *B. bifurcata* will continue to expand throughout the whole of the NW Iberian coast³⁰, whereas the distribution of *Codium* species such as *Codium fragile* subsp. *fragile* (Suringar) Hariot in the NW Atlantic may remain unchanged²⁹. Nevertheless, the physiological effects of increasing temperatures on the cosmopolitan species *C. tomentosum* are unknown.

The aim of this study was to determine the physiological responses of three intertidal macroalgae that are predominant on NW Iberian rocky shores to marine and atmospheric heatwaves during consecutive emersion cycles simulating two spring tidal cycles. We combined field measurements with a novel laboratory experiment in which we recreated the conditions experienced by macroalgae during typical summer consecutive spring tides, where individuals may be exposed to repeated cycles of thermal stress during low tide and to different seawater temperatures. The study evaluated various physiological responses, including mortality rate, growth, photosynthetic performance (as F_v/F_m) and C:N content of *B. bifurcata*, *C. tamariscifolia* and *C. tomentosum* to increased air and seawater temperatures of the magnitude expected under global warming projections. These variables were chosen as suitable proxies for stress because F_v/F_m indicates short-term regulatory responses, whereas growth integrates the intermediate term physiological effects, and the C:N ratio indicates the intermediate term effects on nutrient assimilation and use⁴⁸. We expected to observe lower F_v/F_m and growth⁴⁹, higher C:N ratios⁵⁰, higher probability of mortality³⁷, differences between species due to their different eco-physiological traits⁵¹ and also additive effects of stressors, in response to higher air and seawater temperatures. We also expected cumulative stress to act as a key driver determining different responses of macroalgae to physiological stress.

Results

Field measurements. Environmental conditions. The average seawater temperature recorded by a data logger deployed at the study site in July and August was 17.02 ± 1.05 °C. The day of the field measurements the average seawater temperature was 18.18 ± 0.61 °C, the average amount of light measured on bare rock was 2956 ± 516 μmol photon m⁻² s⁻¹ and the air temperature reached a maximum of 38 °C (Supplementary Fig. S1). The mean temperature below the canopies was 25.68 ± 0.12 °C for *B. bifurcata*, 25.76 ± 0.16 °C for *C. tamariscifolia* and 25.79 ± 0.24 °C for *C. tomentosum*. Humidity (%) below the canopies was 86.13 ± 0.21 for *B. bifurcata*, 86.41 ± 0.29 for *C. tamariscifolia* and 88.27 ± 0.31 for *C. tomentosum*. Temperature below the canopies did not differ between the macroalgae (GLM for temperature: $\chi^2 = 0.15$, df = 2, $p = 0.928$, $n = 3$), whereas humidity was significantly higher below *C. tomentosum* (GLM for humidity: $\chi^2 = 37.49$, df = 2, $p < 0.001$, $n = 3$) (Supplementary Fig. S2).

Δ Weight and $\Delta F_v/F_m$. The weight of the fronds of all three species decreased with increasing air temperature during emersion, although the fronds were not completely dry. After immersion and recovery for 30 min, the weight increased significantly (GEEs: *B. bifurcata*: $\chi^2 = 120$, df = 1, $p < 0.001$; *C. tamariscifolia*: $\chi^2 = 245$, df = 1,

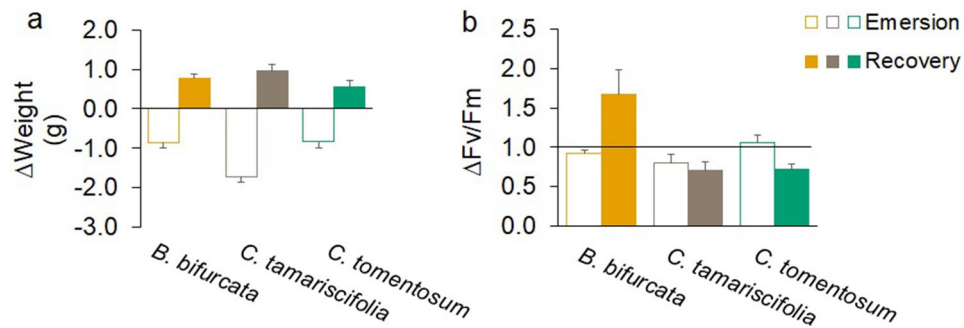


Figure 1. Mean (+SE) value of (a) Δ weight, (b) $\Delta F_v/F_m$ after emersion and recovery in the field measurements.

$p < 0.001$; *C. tomentosum*: $\chi^2 = 15$, $df = 1$, $p < 0.001$) (Fig. 1a), although there were differences between species due to greater weight loss in *C. tamariscifolia*.

The variation in F_v/F_m ($\Delta F_v/F_m$) differed in magnitude between the emersion and recovery periods for *B. bifurcata* (GEE: $\chi^2 = 6.61$, $df = 1$, $p = 0.010$, $n = 10$) and *C. tomentosum* (GEE: $\chi^2 = 111.30$, $df = 1$, $p < 0.001$, $n = 10$), but not for *C. tamariscifolia* (GEE: $\chi^2 = 0.54$, $df = 1$, $p = 0.460$, $n = 10$). After emersion, the change in F_v/F_m was slightly lower than 1 in *B. bifurcata* and *C. tamariscifolia*, whereas in *C. tomentosum* the values of the ratio were above 1 (Fig. 1b). After recovery, *B. bifurcata* showed the greatest change in $\Delta F_v/F_m$ and the value was higher than 1, whereas in *C. tomentosum* the change was smaller and resulted in a reduction in F_v/F_m (Fig. 1b).

Laboratory experiment. Environmental conditions. Light intensity in the immersion tanks was $195 \pm 5 \mu\text{mol photon}\cdot\text{m}^{-2}\text{ s}^{-1}$ and there were no differences between treatments (GLM: $\chi^2 = 7.68$, $df = 2$, $p = 0.020$, $n = 6$). The experimental seawater temperature was 18.45 ± 0.01 °C in control treatments, 19.74 ± 0.02 °C in the marine heatwave treatments and 21.77 ± 0.03 °C in the extreme marine heatwave treatments. Temperatures differed significantly between treatments (GLM: $\chi^2 = 14,621$, $df = 2$, $p < 0.001$, $n = 6$).

During the four hours of emersion in the tanks, the air temperature remained constant in the control treatment, whereas it increased gradually in the atmospheric heatwave and extreme atmospheric heat wave treatments. After the fourth hour in the two emersion cycles, when target temperatures were reached, the temperature under the macroalgal canopies was 22.93 ± 0.08 °C in the control treatment, 28.40 ± 0.19 °C in the heatwave treatment and 30.60 ± 0.14 °C in the extreme heatwave treatment.

The humidity (%) below the canopies after the fourth hour of emersion was 96.15 ± 0.15 in the control treatment, 93.91 ± 0.48 in the heatwave treatment and 91.44 ± 0.90 in the extreme heatwave treatment. The temperatures and the humidity were significantly different among treatments (GLM for temperature: $\chi^2 = 1458.40$, $df = 2$, $p < 0.001$, $n = 6$) (GLM for humidity: $\chi^2 = 32.36$, $df = 2$, $p < 0.001$, $n = 6$) (Supplementary Fig. S3).

Mortality. After the first emersion cycle, dead fronds of all species were observed in the atmospheric heatwave and extreme atmospheric heatwave treatments, although the mortality rates differed between species. The probability curves for mortality in *B. bifurcata* and *C. tomentosum* were similar and showed a lower probability of mortality than those of *C. tamariscifolia* due to the increase in air temperature (Fig. 2a–c). Seawater temperature also had a significant additive effect on the mortality of *C. tamariscifolia* (Table 1) with a significant increase in the probability of mortality in the extreme marine heatwave treatment.

After the second emersion cycle under the control air temperature, dead fronds of *C. tamariscifolia*, but not of *B. bifurcata* or *C. tomentosum*, were observed (Fig. 2d–f). Under the atmospheric heatwave and extreme atmospheric heatwave treatments, the increase in air temperature had a significant effect on *B. bifurcata* mortality, which was much higher in the second than in the first emersion cycle, indicating cumulative effects (Fig. 2d). As in the first emersion cycle, seawater and air temperatures had a significant additive effect on *C. tamariscifolia* mortality (Table 1). The probability of mortality increased under the extreme marine heatwave conditions compared to the control, and it also increased when air temperature increased in the atmospheric heat wave treatment, indicating cumulative effects in the second emersion cycle (Fig. 2e). Air temperature had a marginal effect on *C. tomentosum* mortality (Table 1, Fig. 2f). No dead fronds of any of the species were recorded after the recovery period.

Growth. During the 12-day period of acclimatization to the experimental seawater temperatures, the growth of *C. tamariscifolia* and *C. tomentosum* was greater than that of *B. bifurcata* (Fig. 3a–c). Growth of the three species decreased significantly as the seawater temperature increased (GLMs: *B. bifurcata*: $\chi^2 = 7.58$, $df = 2$, $p < 0.05$, $n = 30$; *C. tamariscifolia*: $\chi^2 = 32.46$, $df = 2$, $p < 0.001$, $n = 30$; *C. tomentosum*: $\chi^2 = 21.37$, $df = 2$, $p < 0.001$, $n = 30$).

After the first emersion cycle, the increase in air temperature significantly affected the growth of *B. bifurcata* and *C. tomentosum* (Table 1). At the control air temperature, the weight of *C. tamariscifolia* decreased, whereas the weight of *B. bifurcata* and *C. tomentosum* remained unchanged. In the atmospheric heatwave and extreme atmospheric heatwave treatments, the weight of all three species decreased, with *C. tamariscifolia* showing the greatest decrease, followed by *C. tomentosum* and *B. bifurcata* (Fig. 3d–f). Because of the high mortality rate,

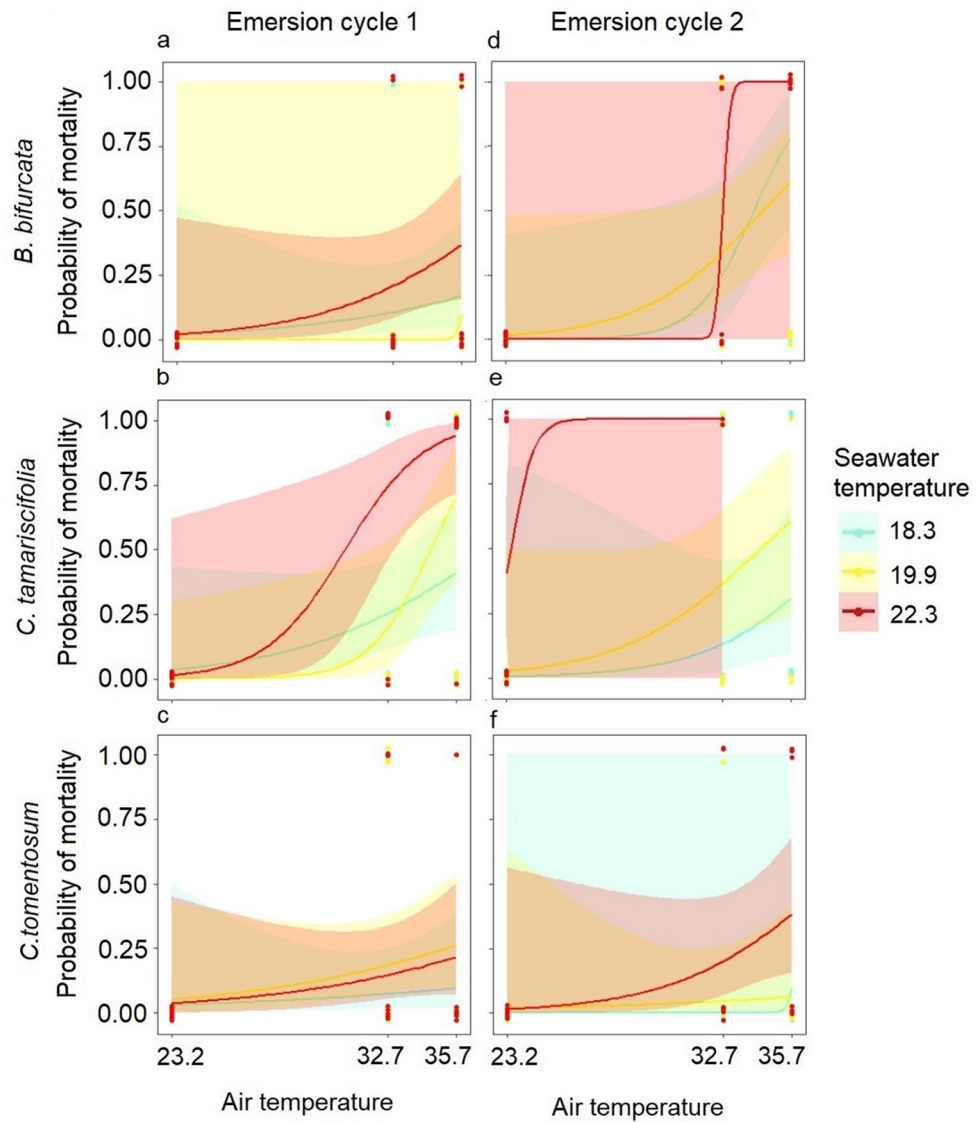


Figure 2. Mortality probability in relation to air and seawater temperature after each emersion cycle in the laboratory experiment. Curves are fitted by GLMs with a binomial error structure and a confidence interval of 95%. Dots indicate binary mortality observations in each treatment (air temperature, control ~ 23.2 °C, atmospheric heatwave ~ 32.7 °C and extreme atmospheric heatwave ~ 35.7 °C), (seawater temperature, control ~ 18.3 °C, marine heatwave ~ 19.9 °C and extreme marine heatwave ~ 22.3 °C).

which resulted in an insufficient number of replicates, the effect of air temperature on the growth of *C. tamariscifolia* could not be modelled, although the trend was for a marked decrease in growth.

After the second emersion cycle, the growth of *B. bifurcata* and *C. tomentosum* decreased significantly as the air temperature increased (Table 1). Growth of the three species at the control air temperature was similar to that observed after the first emersion cycle. In the atmospheric heatwave and extreme atmospheric heatwave treatments, the greatest decrease in growth occurred in *C. tamariscifolia*, followed by *C. tomentosum* and *B. bifurcata* (Fig. 3g–i). The increase in air temperature during consecutive emersion cycles had a cumulative negative effect on the growth of *C. tamariscifolia*. This trend was clearly evidenced in those fronds at the control seawater temperature (18.3 °C), which presented a steeper negative slope after the second emersion (Fig. 3e,h).

After the recovery period, the fronds of *B. bifurcata* and *C. tomentosum* subjected to an increase in water temperature and previously exposed to an increase in air temperature still showed a significant additive effect that led to a decrease in growth (Table 1). Although the fronds of *C. tamariscifolia* and *C. tomentosum* in the control seawater temperature treatment grew, the growth did not compensate for the previous weight loss during the emersion stress. The weight of *C. tamariscifolia* and *C. tomentosum* exposed to the extreme marine heatwave was still lower after the recovery period (Fig. 3j–l).

	Emersion cycle 1			Emersion cycle 2			Recovery		
	χ^2	df	<i>p</i>	χ^2	df	<i>p</i>	χ^2	df	<i>p</i>
Mortality									
<i>B. bifurcata</i>									
ST	4.49	2	0.106	0.69	2	0.707	n.a.		
AT	9.01	2	0.011*	43.38	2	<0.001	n.a.		
STxAT	1.84	4	0.766	3.95	4	0.413	n.a.		
<i>C. tamariscifolia</i>									
ST	12.65	2	<0.010	15.54	2	<0.001	n.a.		
AT	42.07	2	<0.001	13.23	1	<0.001	n.a.		
STxAT	3.82	4	0.430	0.00	2	1	n.a.		
<i>C. tomentosum</i>									
ST	1.55	2	0.461	4.81	2	0.091	n.a.		
AT	15.49	2	<0.001	7.09	2	0.029*	n.a.		
STxAT	0.84	4	0.932	3.20	4	0.524	n.a.		
Growth									
<i>B. bifurcata</i>									
ST	3.72	2	0.156	0.35	2	0.838	24.39	2	<0.001
AT	58.96	2	<0.001	65.99	1	<0.001	18.07	1	<0.001
STxAT	5.48	4	0.241	2.76	2	0.251	8.00	2	0.018*
<i>C. tamariscifolia</i>									
ST	1.53	2	0.465	7.24	2	0.027*	2.39	2	0.302
<i>C. tomentosum</i>									
ST	1.75	2	0.417	0.63	2	0.729	14.65	2	<0.001
AT	60.19	2	<0.001	58.48	2	<0.001	21.22	2	<0.001
STxAT	5.07	4	0.279	1.25	4	0.869	3.96	4	0.411
$\Delta F_v/F_m$									
<i>B. bifurcata</i>									
ST	2.35	2	0.309	0.04	2	0.980	0.97	2	0.616
AT	6.33	2	0.042*	0.69	1	0.405	4.02	1	0.045*
STxAT	8.58	4	0.072	0.69	2	0.706	2.59	2	0.274
<i>C. tamariscifolia</i>									
ST	7.27	2	0.026*	0.87	2	0.648	0.64	2	0.723
<i>C. tomentosum</i>									
ST	2.52	2	0.283	0.19	2	0.907	2.08	2	0.353
AT	0.08	2	0.962	11.47	2	0.003	0.49	2	0.782
STxAT	9.64	4	0.047*	2.83	4	0.587	8.41	4	0.078

Table 1. The summarised results of GLMs used to test the effects of seawater (ST) and air temperature (AT) on the mortality, growth and $\Delta F_v/F_m$ of fronds after the emersion cycles and during the recovery period, in the laboratory experiment. Significant effects ($p < 0.01$) are indicated in bold. * indicates marginal significance. “n.a.” indicates not analysed as no mortality was recorded in the recovery period. Note that due to an insufficient number of replicates, the effect of the extreme atmospheric heatwave (35.7 °C) on the growth and the $\Delta F_v/F_m$ of *B. bifurcata* after the second emersion cycle was not modelled. Likewise, the effect of air temperature on the growth and the $\Delta F_v/F_m$ of *C. tamariscifolia* after the cycles of emersion were not modelled.

$\Delta F_v/F_m$. The photosynthetic performance of the three species decreased when the fronds were subjected to atmospheric heatwave and extreme atmospheric heatwave treatments, as shown by the change in F_v/F_m , with values well below 1, especially in *C. tamariscifolia* (Fig. 4a–f). After the first emersion cycle, under control air temperature, the change in F_v/F_m was similar in *B. bifurcata* and *C. tomentosum* and was slightly higher in *C. tamariscifolia*, with a value below 1. Under atmospheric heatwave and extreme atmospheric heatwave treatments, the change in F_v/F_m was minimal in *C. tomentosum* ($\Delta F_v/F_m \sim 1$), and the $\Delta F_v/F_m$ changed very little in *B. bifurcata*, to values slightly below 1. *Cystoseira tamariscifolia* showed the most marked variation in $\Delta F_v/F_m$, (Fig. 4b), with the F_v/F_m being markedly lower after emersion than prior to emersion. The effect of extreme atmospheric heatwave on the $\Delta F_v/F_m$ in *C. tamariscifolia* could not be modelled, because of the insufficient number of replicates caused by the high mortality. However, the increase in seawater temperature had a marginally significant effect on the variation in $\Delta F_v/F_m$ in *C. tamariscifolia*, for which values were below 1 in the marine heatwave and extreme marine heatwave treatments (Table 1, Fig. 4b).

After the second emersion cycle at control air temperature, the values of $\Delta F_v/F_m$ in *C. tomentosum* and *B. bifurcata* were higher than 1, indicating an increase relative to the pre-emersion values, whereas the $\Delta F_v/F_m$ in

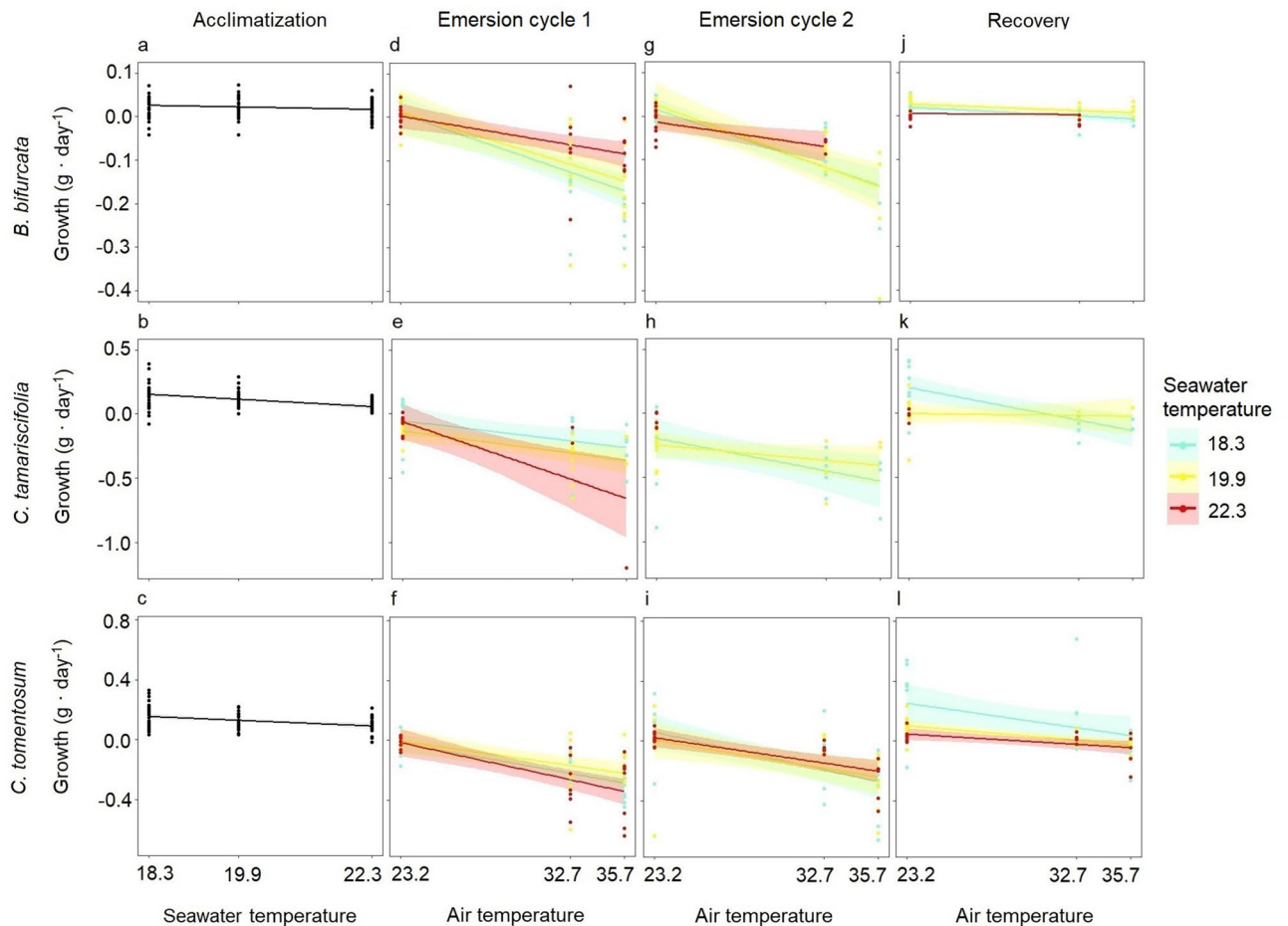


Figure 3. Trends in macroalgal growth as a function of temperature treatments (air temperature: control ~ 23.2 °C, atmospheric heatwave ~ 32.7 °C and extreme atmospheric heatwave ~ 35.7 °C; seawater temperature: control ~ 18.3 °C, marine heatwave ~ 19.9 °C and extreme marine heatwave ~ 22.3 °C) after acclimatization to seawater temperature (a–c), after emersion cycles (d–i) and after recovery (j–l) in the laboratory experiment. The points represent replicates and the smoothed curves are the data fitted by GLMs with a confidence interval of 95%. Note that due to an insufficient number of replicates, the effect of the highest air temperature (35.7 °C) on the growth of *B. bifurcata* after the second emersion cycle was not formally modelled. Likewise, the effect of air temperature on the growth of *C. tamariscifolia* after the two emersion cycles was not formally modelled.

fronds of *C. tamariscifolia* was ~ 1, indicating no variation in F_v/F_m . Under atmospheric heatwave and extreme atmospheric heatwave treatments, the $\Delta F_v/F_m$ tended to change in the three species, to values below 1, when air temperature increased (Fig. 4d–f), although this factor only significantly affected the $\Delta F_v/F_m$ of *C. tomentosum* (Table 1). The consecutive exposure to high air temperature had a cumulative effect on the decrease in photosynthetic performance in *C. tomentosum* (Fig. 4f).

After recovery in immersion tanks, at control seawater temperature, $\Delta F_v/F_m$ varied notably in fronds of *C. tamariscifolia*, indicating that after recovery, the F_v/F_m values exceeded those values before this period, whereas $\Delta F_v/F_m$ in *B. bifurcata* and *C. tomentosum* remained around 1, indicating no recovery of the F_v/F_m values (Fig. 4 g–i). In the marine heatwave treatment (~ 19.9 °C), the $\Delta F_v/F_m$ in *C. tamariscifolia* fronds differed markedly from that in fronds in control seawater, implying the absence of recovery and additional loss of F_v/F_m . By contrast, in marine heatwave and extreme marine heatwave conditions, $\Delta F_v/F_m$ scarcely varied in *C. tomentosum* and increased only slightly in *B. bifurcata* (Fig. 4g,i). The overall change in F_v/F_m after recovery was slight, and the greatest increase (1.5-fold) appeared in *C. tamariscifolia* previously subjected to atmospheric heatwave conditions (air temperature = 32.7 °C).

C:N ratio. The C:N ratio was highest in fronds of *B. bifurcata*, followed by those of *C. tamariscifolia* and *C. tomentosum* (Fig. 5). In general, the C:N ratio increased as the seawater temperature increased (Table 2, Fig. 5), whereas air temperature had only a marginally significant effect on the C:N ratio in *B. bifurcata*. More specifically, the increase in seawater temperature led to a significant decrease in %N in all three macroalgae (Table 2, Fig S4). By contrast, the increase in air temperature tended to decrease the %C in *B. bifurcata* and *C. tomentosum* (Table 2, Supplementary Fig. S4). Air and seawater temperature interacted in the C:N ratio in *C. tomentosum* as

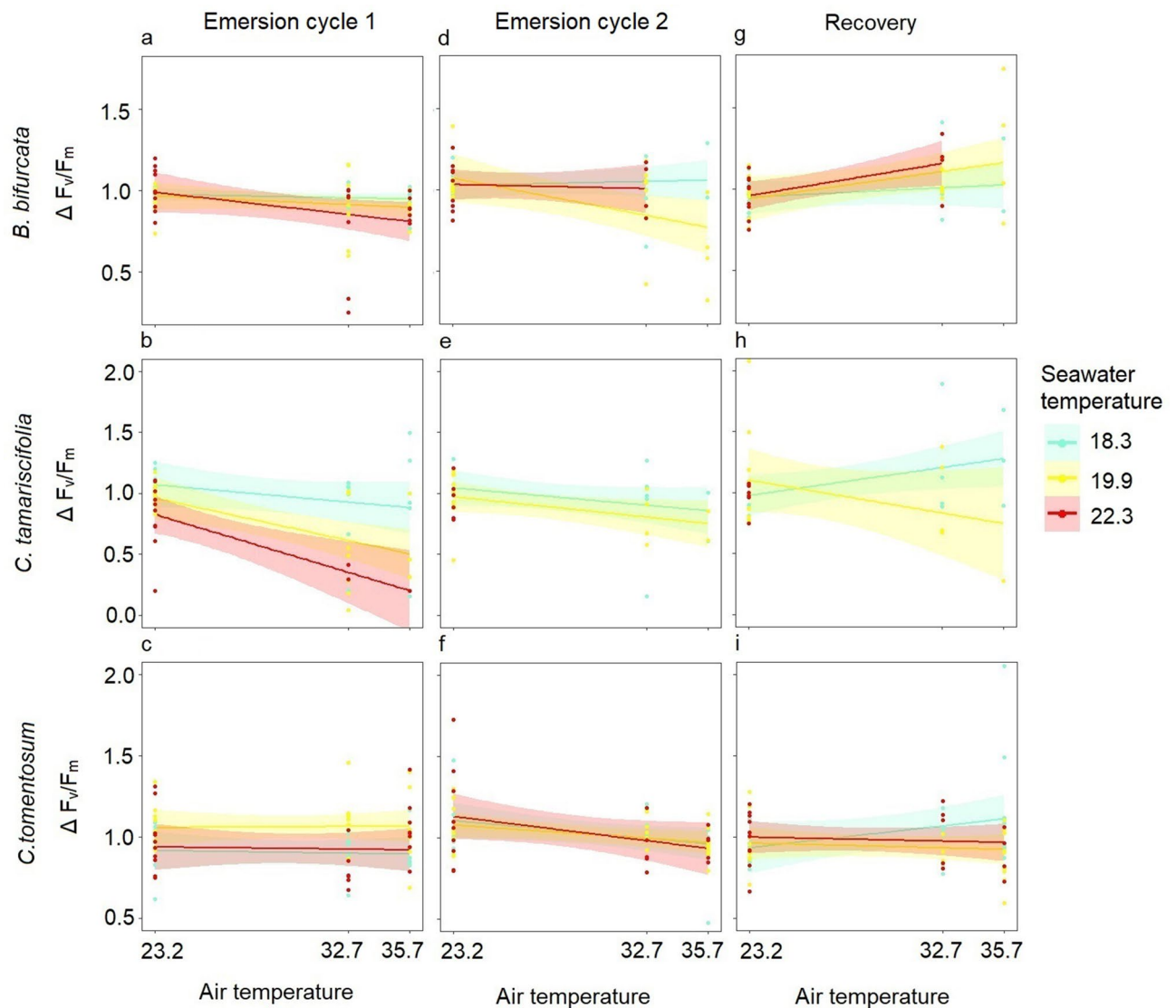


Figure 4. Trends in $\Delta F_v/F_m$ as a function of temperature treatments (air temperature: control ~ 23.2 °C, atmospheric heatwave ~ 32.7 °C and extreme atmospheric heatwave ~ 35.7 °C; seawater temperature: control ~ 18.3 °C, marine heatwave ~ 19.9 °C and extreme marine heatwave ~ 22.3 °C) after the emersion cycles (a–f) and recovery periods (g–i) in the laboratory experiment. The points are the replicates and the smoothed curves are the data fitted by GLMs with a confidence interval of 95%. Note that due to an insufficient number of replicates, the effect of the highest air temperature level (35.7 °C) on the $\Delta F_v/F_m$ of *B. bifurcata* after the second emersion cycle was not formally modelled. Likewise, the effect of air temperature on the $\Delta F_v/F_m$ of *C. tamariscifolia* after the two emersion cycles was not formally modelled.

the C:N ratio tended to increase as the seawater temperature increased, although the trend was less marked in fronds exposed to higher air temperature during emersion cycles (note the less steep slopes for air temperatures of 32.7 and 35.7 °C in Fig. 5c).

Discussion

This study showed that the stressful conditions created particularly by atmospheric heatwaves and, to less extent, by marine heatwaves negatively affected the survival and physiology of intertidal macroalgae after exposure to two consecutive emersion cycles, and that these stressors had an additive effect. Increased air temperature caused important negative short- and intermediate-term effects on the physiological performance of the macroalgae in the field and the laboratory experiment, effects that were cumulative after exposure to two consecutive emersion cycles in the laboratory experiment. This pattern is consistent with the findings of other studies in which air temperature was found to be a relevant factor modulating physiological stress in intertidal macroalgae^{6,15,20,26,37} and of others that related contractions in the distribution of intertidal macroalgae to large increases in air temperature^{37,52,53}. The seawater temperatures applied in the laboratory experiment (which reflected realistic present and future climatic scenarios according to historic databases, scientific literature and IPCC predictions) were below the physiological threshold of 23 °C for *B. bifurcata*⁵⁴. The highest temperature was above

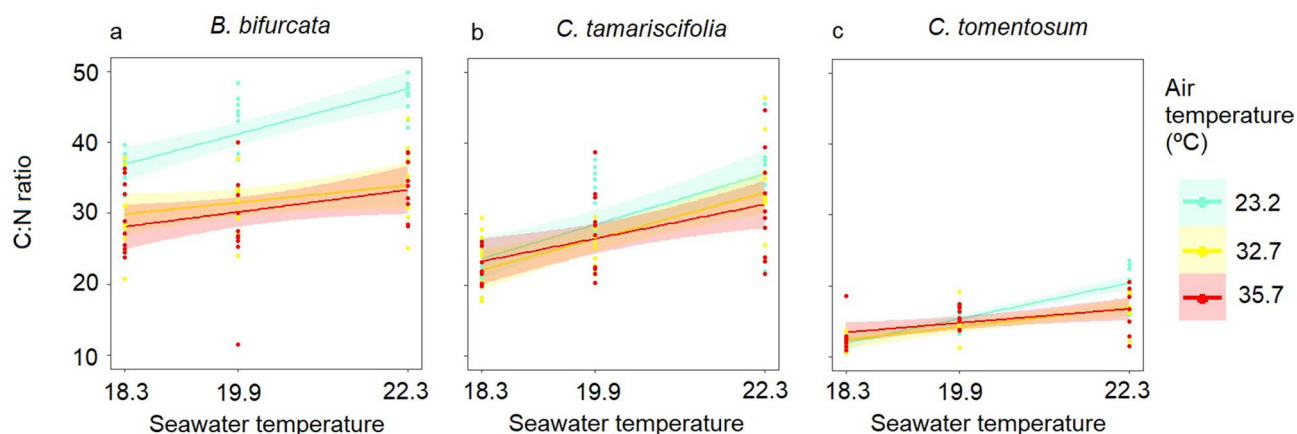


Figure 5. C:N ratio as a function of seawater temperature treatments (control ~ 18.3 °C, marine heatwave ~ 19.9 °C and extreme marine heatwave ~ 22.3 °C) in fronds exposed to control (~ 23.2 °C), atmospheric heatwave (~ 32.7 °C) and extreme atmospheric heatwave (~ 35.7 °C) air temperatures during emersion. The points are the replicates and the smoothed curves are the data fitted by GLMs with a confidence interval of 95%.

	<i>B. bifurcata</i>			<i>C. tamariscifolia</i>			<i>C. tomentosum</i>		
	χ^2	df	<i>p</i>	χ^2	df	<i>p</i>	χ^2	df	<i>p</i>
C:N ratio									
ST	28.26	2	<0.001	33.81	2	<0.001	96.19	2	<0.001
AT	8.15	2	0.017*	0.50	2	0.777	2.01	2	0.366
ST x AT	13.04	4	0.011*	9.91	4	0.042	18.11	4	0.001
C %									
ST	6.48	2	0.039*	9.48	2	<0.01	2.27	2	0.321
AT	67.35	2	<0.001	0.86	2	0.651	7.25	2	0.026*
ST x AT	4.49	4	0.344	1.51	4	0.827	5.81	4	0.214
N %									
ST	9.77	2	0.007	53.29	2	<0.001	93.99	2	<0.001
AT	16.99	2	<0.001	1.62	2	0.446	2.68	2	0.261
ST x AT	6.57	4	0.160	8.84	4	0.065	14.14	4	0.007

Table 2. The summarised results of GLMs testing the effects of seawater (ST) and air (AT) temperature on the C:N ratio, C% and N% of the fronds after the low tides and the recovery in the laboratory experiment. Significant effects ($p < 0.01$) are shown in bold. * indicates marginal significance.

the optimum for net photosynthesis in *B. bifurcata* and *C. tamariscifolia* (20.56 ± 1.94 °C and 21.9 ± 1.13 °C, respectively)⁵⁵. Thus, the increased seawater temperatures negatively affected the physiological performance of fronds, but led to sub-lethal effects.

The different indicators measured in macroalgae after the emersion cycles showed a consistent decline of the physiological performance caused by atmospheric and marine heatwaves, which was greater under the most extreme conditions, i.e. global warming scenario. The F_v/F_m ratio reflected short term regulatory mechanisms such as photoprotection⁵⁶, whereas the changes in growth and the C:N ratio integrated physiological processes over longer periods⁴⁸. Values of $\Delta F_v/F_m$ much lower than 1, caused by the high air temperature, suggest short-term regulatory effects on the physiology of macroalgae and were probably a consequence of desiccation and thermal stress. Tissue desiccation tends to decrease the F_v/F_m , due to a diminution of osmotic potential^{18,49,52,57,58}, affects photosynthesis, C fixation and generates overproduction of reactive oxygen species (ROS)^{23,59,60} with negative consequences on physiological processes^{23,57,59,61}, and the high temperatures also cause enzyme denaturalization^{59,62}. The macroalgae resist this disruptive stress and prevent lethal damage by reducing all metabolic activities^{63,64}, thereby inhibiting growth⁴⁹. This capacity was evidenced by the survival of the large proportion of fronds that suffered severe desiccation and also the increased weight and F_v/F_m observed after recovery. The increasing seawater temperature also increased significantly the C:N ratio, as previously observed in diverse red and brown seaweeds⁵⁰. This increase occurred as a consequence of significant decreases in %N (Table 2, Supplementary Figure S4) coincident with patterns observed in laminarians⁶⁵. Higher seawater temperatures have often been linked to a decrease in the activity of nitrate reductase in intertidal and subtidal macroalgae^{66,67}, implying a lower assimilation capacity of NO_3^- and lower incorporation rates of N. The above-mentioned effects, together with the cumulative stress caused by two consecutive cycles of emersion under

atmospheric heatwaves, probably overwhelmed the shelf-shading protective mechanisms of the canopies against desiccation^{6,13,14,52,68}, the production of heat shock proteins and the repair processes^{10,23,48,59}, and prevented the fronds from recovering the pre-stress F_v/F_m and weight, leading to death in some cases as evidenced by the cumulative mortality in *C. tamariscifolia* and *B. bifurcata*. This may result in a decline of the abundance of these habitat-forming macroalgae in the intertidal, as reported in³⁷.

The species under study showed different capacities to tolerate increase in air temperature, with *C. tamariscifolia* being the most vulnerable and *C. tomentosum* the most resistant and resilient. The high resilience of *C. tomentosum* was indicated by the recovery of F_v/F_m to pre-stress values, although the second emersion weakened this capacity suggesting cumulative stress. The decrease in F_v/F_m in *B. bifurcata* after emersion in the field was followed by a large increase in F_v/F_m after the recovery period, revealing the resilience of this alga after moderate desiccation. Moreover, in *C. tomentosum* and *B. bifurcata*, the F_v/F_m changed little, with values slightly higher than 1 obtained after the second laboratory emersion experiment at control air temperature. This suggests that after moderate desiccation, the water loss was not high enough to alter the efficiency of charge separation during photosynthesis^{18,58}, indicating the absence of a high level of physiological stress. The morphological traits also influence resistance to desiccation⁶⁸. The desiccation rate is lower in the thick and voluminous fronds of *C. tomentosum*, which have a smaller specific surface than the fronds of *C. tamariscifolia*^{10,69}. In comparison to *C. tamariscifolia*, the less pronounced decrease in growth observed in *B. bifurcata* after the two emersion cycles was mainly a consequence of a slower growth rate⁵¹. The different resistance and resilience to increasing air temperatures might imply a change in the structure of macroalgal assemblages on intertidal rocky shores of NW Spain under global warming scenarios, with an increase in the relative abundance of *C. tomentosum* and *B. bifurcata* and a decrease in *C. tamariscifolia*.

Although experimental and field responses showed similar patterns, extrapolation of laboratory results to the field must be done with caution. In the laboratory experiment, the humidity levels were higher than in the intertidal, which implies that emersions under the same conditions at the intertidal could lead to stronger negative effects such as higher desiccation, lower physiological performance and greater mortality. By contrast, the irradiance levels in the laboratory were much lower than those experienced in the intertidal, and might have been below the saturation points (I_k) of the species, as for example the I_k of the intertidal furoid *Fucus spiralis* is above 300 $\mu\text{mol photon m}^{-2} \text{s}^{-1}$ under emersion with air temperatures of 20°C²². This light limitation might result in lower photosynthetic efficiency and smaller growth rates during the laboratory experiment with potentially more intense negative effects of the desiccation during emersions²² and inhibition of the recovery responses during immersions (see⁷⁰). Nevertheless, our results might have broader consequences for the future geographical distribution of macroalgae. The NW Iberian Peninsula represents the range center of the species studied (www.marinespecies.org; www.obis.org)⁷¹. In this area, previous studies have predicted an expansion and increase in the abundance of *B. bifurcata*, *C. tamariscifolia* and *Codium* spp. in response to the increased sea surface temperature expected under global warming scenarios (see [Introduction](#)). However, the present findings show that atmospheric heatwaves during low tide may be detrimental to the performance and survival of these species, probably inhibiting the predicted shifts. The importance of air temperature for the habitat suitability of intertidal macroalgae is evident; however, species distribution models (SDMs) and databases that take air temperature into account^{72–74} are scarcer than models including only seawater temperature. To improve the forecasting of potential range shifts in intertidal macroalgae due to global warming, air temperature should be included as a factor in SDMs. Air and seawater temperature acted additively increasing the mortality of *C. tamariscifolia* after emersion cycles and decreasing the growth of *B. bifurcata* and *C. tomentosum* after a period of recovery. These additive effects coincide with patterns observed in other intertidal macroalgae²⁰, probably because both factors affect similar physiological mechanisms⁷⁵.

The fact that the macroalgae exposed to atmospheric heatwaves during two consecutive cycles of emersion suffered cumulative effects on their physiological performance and mortality is important, as air temperature and the frequency of heatwaves are expected to increase under global warming scenarios predicted for the region^{8,9}. A decline in these bio-engineering macroalgae may remove habitat and shelter for several species in higher trophic levels, degrading the benthic community and having negative consequences on diversity and fisheries³³. Future experiments could apply higher-resolution air temperature gradients to intertidal macroalgae to obtain data for constructing thermal physiological performance curves, especially under consecutive periods of exposure at low tide. Despite the limitations of laboratory experiments, their contribution to assessing the cumulative effects of chronic exposure to atmospheric heatwaves during low tide is crucial, as the findings can help to improve predictive models that forecast the effects of global warming on the physiology and distribution of ecologically important intertidal macroalgae.

Materials and methods

Field measurements. The field measurements were carried out on 4 August 2019 at noon during low spring tide to examine the effects of air temperature on the photosynthetic performance and wet weight of the co-occurring species *B. bifurcata*, *C. tamariscifolia* and *C. tomentosum* in situ. These species coexist at the middle intertidal zone on the Isle of Monteaudo (area surrounding coordinates 42.23551°N, 8.89956°W), which belongs to the Cíes Islands archipelago, which forms part of the Atlantic Islands of Galicia National Park (NW Iberian Peninsula; Fig. 6). The study site is located in the Ría de Vigo, which experiences mesotidal semi-diurnal tides. At this site, the target species cover wide areas of the mid intertidal zone, forming dense, bushy canopies that emerge during an average of 4 h under low spring tides under favourable conditions (high atmospheric pressure and low wave height).

On the day that the field measurements were conducted, the insolation was 76.8%, the average wind speed was 6 km/h, and the average air temperature was 19 °C (www.meteogalicia.gal).

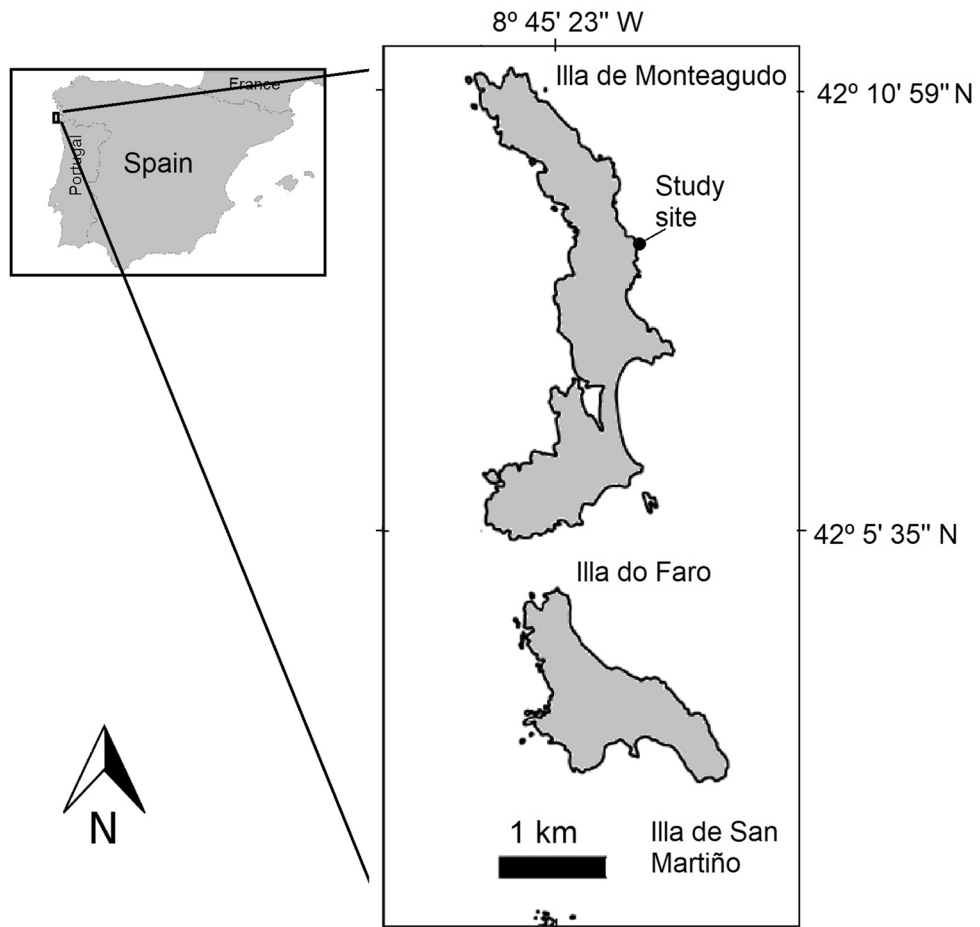


Figure 6. Location of the field measurements and the rocky intertidal sampling site on the Cíes Islands (Atlantic Islands of Galicia National Park, NW Spain). Map derived from BDLJE CC-BY 4.0 www.scne.es, modified with QGIS 3.4.5. software (www.qgis.org).

A HOBO Pendant temp/light data logger (Onset Computer Corp., Bourne, MA, USA) with an accuracy range of ± 0.53 °C and resolution of 0.14 °C placed on the bare rock recorded light and temperature data every 5 min. In addition, three temperature and humidity iButton Hygrochron data loggers (Maxim Integrated Products, Dallas Semiconductor, USA) with an accuracy range of ± 0.50 °C and resolution of 0.0625 °C placed below the canopy of each species (total N = 9) recorded data every minute.

The physiological responses of the macroalgae were assessed after emersion during low tide and subsequent recovery by immersion in seawater. Once the tide ebbed, 10 fronds of each species (N = 30) were cut from the canopies, numbered and weighed to determine the pre-stress wet weight. The fronds were then dark adapted with two layers of thick opaque plastic for 30 min to allow the complete oxidation of reaction centers for determining basal fluorescence (F_0). The maximum quantum yield of photosynthesis (F_v/F_m) was then measured in the central part of the fronds with a Pulse-Amplitude-Modulation (PAM) chlorophyll fluorometer. The fronds were held under direct sunlight for two hours and then were dark-adapted for 30 min, and the F_v/F_m and wet weight were again determined. The recovery treatment was applied by placing the fronds in a bucket filled with seawater and covered with opaque plastic for 30 min, before repeating wet weight and F_v/F_m measurements.

The variation in photosynthetic performance ($\Delta F_v/F_m$) was calculated using Eq. (1):

$$\Delta \frac{F_v}{F_m} = \frac{(F_v/F_m)_{\text{after treatment}}}{(F_v/F_m)_{\text{before treatment}}} \quad (1)$$

This ratio was used to evaluate the physiological condition of macroalgae, where values > 1 indicate an increase in the F_v/F_m , i.e. improved performance, and values < 1 indicate a decrease in F_v/F_m , i.e. poorer performance after the treatments. The variation in weight (ΔWeight) indicated the potential for desiccative water loss under emersion in the field, which is linked to the different physiological responses of each species under desiccation stress. ΔWeight was calculated in the same way as $\Delta F_v/F_m$.

Laboratory experiment. A laboratory experiment was performed between 18 June and 26 July 2019 to assess the effects of air and seawater temperatures on the physiological performance of macroalgae. The experimental set-up included Species (3 levels: *B. bifurcata*, *C. tamariscifolia* and *C. tomentosum*), Seawater temperature (3 levels: control ~ 18.3 °C, marine heatwave ~ 19.9 °C and extreme marine heatwave ~ 22.3 °C) and Air temperature during the emersion periods (3 levels: control ~ 22.3 °C, atmospheric heatwave ~ 32.7 °C and extreme atmospheric heatwave ~ 35.7 °C) as fixed orthogonal factors (n = 10). The seawater and air temperature treatments used in this experiment were selected to simulate realistic present and future situations according to baseline scenarios in which the current trends in greenhouse gas emissions remain unaltered⁷.

Control seawater temperature was the average ambient summer temperature in July and August between 2009 and 2018 at the nearby Baiona coastal station in the Ría de Vigo (<http://www.intecmar.gal/MultiParam/Default.aspx>); the marine heatwave temperature was the average of values higher than the 95th percentile of the records; and the extreme marine heatwave temperature was the marine heatwave temperature under a future scenario of global warming, with a 2.4 °C increase for the Iberian upwelling in the 2070–2100 period⁴¹. The emersion air temperatures corresponded to average air temperatures at noon on the Cíes Islands in July and August between 2009 and 2018 (www.meteogalicia.gal). Control air temperature was the average summer temperature at noon; atmospheric heatwave temperature was the average temperature at noon above the 95th percentile, recorded on more than three days (www.aemet.es); and the extreme atmospheric heatwave temperature represented a heatwave under a global warming scenario of a 3.0 °C increase. This increase is the average calculated from the predictions of baseline scenarios for the period 2081–2100⁷.

A total of 270 vegetative fronds (90 fronds per each species) were collected in the middle intertidal zone (Fig. 6) and transported to the Estación de Ciencias Mariñas de Toralla (ECIMAT) facilities, which form part of the Marine Research Centre (CIM) of the University of Vigo (Spain). The fronds were acclimated for 6 days to laboratory conditions to enable a steady growth response to be reached. All fronds were numbered, attached to nylon strings inside two 100 L tanks and immersed in running filtered (50 µm) seawater at 16 °C under the ambient 15:9 photoperiod typical of June. To simulate the average seawater temperatures experienced in the region in summer (~ 18 °C), the temperature of the seawater in the tanks was increased gradually over three days, by decreasing the 16 °C water flux and increasing the 18 °C water flux.

After acclimatization at 18 °C, the fronds were placed in 35L tanks with an open circulating system within an isothermal walk-in chamber at ~ 20 °C. Each seawater temperature was assigned to two tanks (total N = 6 tanks). The desired seawater temperatures were achieved by heating the 18 °C seawater with titanium aquarium heaters (100 W) inside head tanks, which supplied the heated water to other tanks containing the fronds. Heated water was mixed with water at 18 °C, and both fluxes were gradually regulated to increase the temperature at a rate of 1 °C per day. The fronds were acclimatized to the seawater temperatures for 12 days. In each tank, 15 fronds of each species were randomly placed and exposed to summer photoperiod conditions of 15:9 h light: darkness (Supplementary Fig. S5). Light was supplied from above by LED lamps. To prevent any effects due to differences in light within the tanks, the fronds were moved to different positions in each tank every 2 days. To minimize any effects of the tank, fronds were moved every 5 days between tanks containing seawater at the same temperature.

After the acclimatization period, the fronds were subjected to a daily emersion period of 4 h (from 10:00 to 14:00) simulating low spring tides, during 3 consecutive days. The fronds were then subjected to an immersion period (8 days) simulating neap tides and then to another period of 3 consecutive days with a daily emersion of 4 h. After the second emersion period, fronds were again submerged in seawater for 6 days at the respective seawater temperatures to check their recovery. The laboratory experiment lasted for 38 days in total (Supplementary Fig. S6).

During emersion, fronds were transferred from the seawater tanks to tanks containing moistened granite tiles (natural rocky substrata of the algae in the field) placed on shelves inside the same chamber for 4 h, i.e. average emersion time experienced by macroalgae in the mid intertidal zone during spring tides at the sampling site. The fronds were distributed in layers (fronds covering other fronds) simulating their natural distribution in the field. The emersion tanks were lit from above by LED lamps, with the same light intensity and photoperiod as in the seawater tanks. The air temperature was increased gradually during emersion by using infrared ceramic heaters positioned over the tanks, in which the air was re-circulated with small battery-operated fans. The air temperature was regulated with digital temperature controllers positioned above the canopies. Temperature and humidity during emersion were monitored by data loggers positioned below the canopies.

The response variables mortality, wet weight and F_v/F_m were measured in fronds before each emersion period and 20 h after each (days 18, 22, 29, 33) and after six days of recovery (day 38).

The numbers of dead fronds were recorded. Mortality was considered a binary response variable (1 = dead, 0 = alive). Wet weight was obtained in fronds previously blotted with paper to remove excess water from the surface. Growth was determined as the difference in wet weight 20 h after each treatment and the wet weight before each treatment (emersion cycles 1 and 2/recovery), divided by the number of days, according to²⁰. This calculation enabled to directly assess if there was an increase in weight and net growth (positive values), no increase (zero), or decrease in fronds weight due to losses of tissue (negative values) after the emersions and the recovery. The F_v/F_m was measured before emersion cycles and/or recovery and 20 h later, and the variation in photosynthetic performance ($\Delta F_v/F_m$) was calculated using Eq. (1). The C:N ratio was determined in fronds removed from the tanks at the end of the experiment. The fronds were rinsed repeatedly to remove salts and then ground to produce a fine, homogenous powder. The C:N ratio was determined by CNHS elemental microanalysis (in a Fisons Carlo Erba EA1108 elemental analyser) at the analytical facilities of the University of Vigo (CACTI-UVIGO).

Data analysis. The responses of each species to environmental factors in the field measurements and the laboratory experiment were analysed separately due to expected species-specific responses.

To determine whether the Δ weight and $\Delta F_v/F_m$ in species differed between treatments in the field, generalized estimating equation models (GEEs) were used, with Treatment (2 levels: emersion vs. recovery) as a fixed factor. GEEs estimate the regression parameters considering the correlation between observations in clustered data⁷⁶. The GEEs had an autoregressive correlation structure and a Gaussian error distribution.

Between-species differences in temperature and humidity in the field were tested using a general linear model (GLM) including Species (3 levels: *B. bifurcata*, *C. tamariscifolia* and *C. tomentosum*) as a fixed factor. In the laboratory experiment, GLMs were also used to test for any differences in seawater temperature and light between the immersion tanks, as well as for differences in air temperature and humidity between the emersion tanks.

To determine whether mortality, growth, $\Delta F_v/F_m$ and C:N ratio differed between treatments in the laboratory experiment, the GLMs included Air temperature (3 levels: control ~ 22.3 °C, atmospheric heatwave ~ 32.7 °C and extreme atmospheric heatwave ~ 35.7 °C) and Seawater temperature (3 levels: control ~ 18.3 °C, marine heatwave ~ 19.9 °C and extreme marine heatwave ~ 22.3 °C) as fixed orthogonal factors. Mortality data were fitted by GLMs with a binomial error structure, whereas growth, $\Delta F_v/F_m$ and C:N ratio data were fitted by GLMs with a Gaussian error structure. The GLMs were only used when treatment groups (Air temperature x Seawater temperature) included at least 4 observations, because in some cases there was an insufficient number of replicates due to the high mortality rate. Therefore, the models did not include the effect of the highest air temperature (35.7 °C) on the growth and the $\Delta F_v/F_m$ of *B. bifurcata* after the second emersion cycles or the effect of the air temperature factor on the growth or the $\Delta F_v/F_m$ of *C. tamariscifolia* after the two emersion cycles.

When response variables did not fulfil the parametric assumptions, or when the model was unbalanced, a more conservative significance level of $p = 0.01$ was established. The goodness of fit of the models was assessed by graphically checking the error distribution, and the statistical significance of the models was calculated using Chi-square tests⁷⁷. When models were significant, post hoc multiple comparison tests were conducted and Bonferroni p value corrections were applied. All data are reported as means \pm S.E. Statistical analyses were performed with R 3.5.3 software, by using the “geepack” package⁷⁶ for the GEEs and default system packages for the other tests.

Received: 20 May 2020; Accepted: 26 November 2020

Published online: 08 December 2020

References

1. Umanzor, S., Ladah, L. & Calderon-aguilera, L. E. Testing the relative importance of intertidal seaweeds as ecosystem engineers across tidal heights. *J. Exp. Mar. Bio. Ecol.* **511**, 100–107 (2018).
2. Smale, D. A., Burrows, M. T., Moore, P., O'Connor, N. & Hawkins, S. J. Threats and knowledge gaps for ecosystem services provided by kelp forests: a northeast Atlantic perspective. *Ecol. Evol.* **3**, 4016–4038 (2013).
3. Krause-Jensen, D. & Duarte, C. M. Substantial role of macroalgae in marine carbon sequestration. *Nat. Geosci.* **9**, 737–742 (2016).
4. King, N. G., McKeown, N. J., Smale, D. A. & Moore, P. J. The importance of phenotypic plasticity and local adaptation in driving intraspecific variability in thermal niches of marine macrophytes. *Ecography (Cop.)* **41**, 1469–1484 (2018).
5. Helmuth, B., Mieszkowska, N., Moore, P. & Hawkins, S. J. Living on the edge of two changing worlds: forecasting the responses of rocky intertidal ecosystems to climate change. *Annu. Rev. Ecol. Syst.* **37**, 373–404 (2006).
6. Fernández, A. *et al.* Additive effects of emersion stressors on the ecophysiological performance of two intertidal seaweeds. *Mar. Ecol. Prog. Ser.* **536**, 135–147 (2015).
7. IPCC. Summary for Policymakers. In: *Climate Change 2014, Mitigation of Climate Change. Contribution of Working Group III to the Fifth Assessment Report of the Intergovernmental Panel on Climate Change* (eds. Edenhofer, O. *et al.*). (Cambridge University Press, Cambridge, 2014).
8. Meehl, G. A. & Tebaldi, C. More intense, more frequent, and longer lasting heat waves in the 21st century. *Science* **305**, 994–997 (2004).
9. Koffi, B. & Koffi, E. Heat waves across Europe by the end of the 21st century: multiregional climate simulations. *Clim. Res.* **36**, 153–168 (2008).
10. Lüning, K. *Temperature, salinity and other abiotic factors in Seaweeds. Their Environment, Biogeography and Ecophysiology* (Wiley, New York, 1990).
11. Pang, S. J., Jin, Z. H., Sun, J. Z. & Gao, S. Q. Temperature tolerance of young sporophytes from two populations of *Laminaria japonica* revealed by chlorophyll fluorescence measurements and short-term growth and survival performances in tank culture. *Aquaculture* **262**, 493–503 (2007).
12. Nielsen, S. L., Nielsen, H. D. & Pedersen, M. F. Juvenile life stages of the brown alga *Fucus serratus* L. Are more sensitive to combined stress from high copper concentration and temperature than adults. *Mar. Biol.* **161**, 1895–1904 (2014).
13. Schonbeck, M. W. & Norton, T. A. The effects on intertidal fucooid algae of exposure to air under various conditions. *Bot. Mar.* **23**, 141–148 (1980).
14. Pearson, G. A., Lago-Leston, A. & Mota, C. Frayed at the edges: Selective pressure and adaptive response to abiotic stressors are mismatched in low diversity edge populations. *J. Ecol.* **97**, 450–462 (2009).
15. Ferreira, J. G., Arenas, F., Martínez, B., Hawkins, S. J. & Jenkins, S. R. Physiological response of fucooid algae to environmental stress: comparing range centre and southern populations. *New Phytol.* **202**, 1157–1172 (2014).
16. Smale, D. A. & Wernberg, T. Extreme climatic event drives range contraction of a habitat-forming species. *Proc. R. Soc. B.* **280**, 20122829 (2013).
17. Jueterbock, A. *et al.* Thermal stress resistance of the brown alga *Fucus serratus* along the North-Atlantic coast: Acclimatization potential to climate change. *Mar. Genomics* **13**, 27–36 (2014).
18. Hurd, K., Harrison, P. J., Bischof, K. & Lobban, C. S. Light and photosynthesis in *Seaweed Ecology and Physiology* (eds. Hurd, K., Harrison, P. J., Bischof, K. & Lobban, C. S.) 176–237. (Cambridge University Press, Cambridge, 2014).
19. Mota, C. F. *et al.* Differentiation in fitness-related traits in response to elevated temperatures between leading and trailing edge populations of marine macrophytes. *PLoS ONE* **13**, 1–17 (2018).
20. Martínez, B. *et al.* Physical factors driving intertidal macroalgae distribution: physiological stress of a dominant fucooid at its southern limit. *Oecologia* **170**, 341–353 (2012).
21. Pereira, T. R., Engelen, A. H., Pearson, G. A., Valero, M. & Serrão, E. A. Response of kelps from different latitudes to consecutive heat shock. *J. Exp. Mar. Bio. Ecol.* **463**, 57–62 (2015).

22. Madsen, T. V. & Maberly, S. C. A comparison of air and water as environments for photosynthesis by the intertidal alga *Fucus spiralis* (Phaeophyta). *J. phycol.* **26**(1), 24–30 (1990).
23. Contreras-Porcia, L., López-Cristoffanini, Meynard, A., & Kumar, M. Tolerance pathways to desiccation stress in seaweeds. In *Systems Biology of Marine Ecosystems* (eds. Kumar, M. & Ralhp, P.) 13–29. (Springer, Berlin, 2017).
24. Helmuth, B. *et al.* Climate change and latitudinal patterns of intertidal thermal stress. *Science* **298**, 1015–1017 (2002).
25. King, N. G. *et al.* Cumulative stress restricts niche filling potential of habitat-forming kelps in a future climate. *Funct. Ecol.* **32**, 288–299 (2017).
26. Hereward, H. F. R., King, N. G. & Smale, D. A. Intra-annual variability in responses of a canopy forming kelp to cumulative low tide heat stress: implications for populations at the trailing range edge. *J. Phycol.* **56**, 146–158 (2019).
27. Fernández, C. The retreat of large brown seaweeds on the north coast of Spain: the case of *Saccorhiza polyschides*. *Eur. J. Phycol.* **46**, 352–360 (2011).
28. Méndez-Sandín, M. & Fernández, C. Changes in the structure and dynamics of marine assemblages dominated by *Bifurcaria bifurcata* and *Cystoseira* species over three decades (1977–2007). *Estuar. Coast. Shelf Sci.* **175**, 46–56 (2016).
29. Wilson, K. L., Skinner, M. A. & Lotze, H. K. Projected 21st-century distribution of canopy-forming seaweeds in the Northwest Atlantic with climate change. *Divers. Distrib.* **25**, 582–602 (2019).
30. Martínez, B., Viejo, R. M., Carreño, F. & Aranda, S. C. Habitat distribution models for intertidal seaweeds: Responses to climatic and non-climatic drivers. *J. Biogeogr.* **39**, 1877–1890 (2012).
31. Nyström, M. *et al.* Confronting feedbacks of degraded marine ecosystems. *Ecosystems* **15**, 695–710 (2012).
32. O'Brien, B. S., Mello, K., Litterer, A. & Dijkstra, J. A. Seaweed structure shapes trophic interactions: a case study using a mid-trophic level fish species. *J. Exp. Mar. Biol. Ecol.* **506**, 1–8 (2018).
33. Voerman, S. E., Llera, E. & Rico, J. M. Climate driven changes in subtidal kelp forest communities in NW Spain. *Mar. Environ. Res.* **90**, 119–127 (2013).
34. Duarte, L. *et al.* Recent and historical range shifts of two canopy-forming seaweeds in North Spain and the link with trends in sea surface temperature. *Acta Oecol.* **51**, 1–10 (2013).
35. Viejo, R. M., Martínez, B., Arrontes, J., Astudillo, C. & Herna, L. Reproductive patterns in central and marginal populations of a large brown seaweed: drastic changes at the southern range limit. *Ecography* **34**, 75–84 (2011).
36. Duarte, L. & Viejo, R. M. Environmental and phenotypic heterogeneity of populations at the trailing range-edge of the habitat-forming macroalga *Fucus serratus*. *Mar. Environ. Res.* **136**, 16–26 (2018).
37. Thomsen, M. S. *et al.* Local extinction of bull kelp (*Durvillaea* spp.) due to a marine heatwave. *Front. Mar. Sci.* **6**, 1–10 (2019).
38. Darling, E. S. & Côté, I. M. Quantifying the evidence for ecological synergies. *Ecol. Lett.* **11**, 1278–1286 (2008).
39. Gómez-Gesteira, M. *et al.* The state of climate in NW Iberia. *Clim. Res.* **48**, 109–144 (2011).
40. Kersting, D.K. *Cambio Climático en El Medio Marino Español: Impactos, Vulnerabilidad y Adaptación*. Oficina Española de Cambio Climático, Ministerio de Agricultura, Alimentación y Medio Ambiente. Madrid. <http://cort.as/-HXq9> (2016).
41. Philippart, C. J. M. *et al.* Impacts of climate change on European marine ecosystems: observations, expectations and indicators. *J. Exp. Mar. Biol. Ecol.* **400**, 52–69 (2011).
42. Lima, F. P., Ribeiro, P. A., Queiroz, N., Hawkins, S. J. & Santos, A. M. Do distributional shifts of northern and southern species of algae match the warming pattern?. *Glob. Chang. Biol.* **13**, 2592–2604 (2007).
43. Díez, I., Muguerza, N., Santolaria, A., Ganzedo, U. & Gorostiaga, J. M. Seaweed assemblage changes in the eastern Cantabrian Sea and their potential relationship to climate change. *Estuar. Coast. Shelf Sci.* **99**, 108–120 (2012).
44. Piñeiro-Corbeira, C., Barreiro, R. & Cremades, J. Decadal changes in the distribution of common intertidal seaweeds in Galicia (NW Iberia). *Mar. Environ. Res.* **113**, 106–115 (2016).
45. García-Fernández, A. & Bárbara, I. Studies of *Cystoseira* assemblages in Northern Atlantic Iberia. *Ann. del Jard. Bot. Madrid* **73**, 1–21 (2016).
46. García, A. G., Olabarria, C., Arrontes, J., Álvarez, Ó. & Viejo, R. M. Spatio-temporal dynamics of *Codium* populations along the rocky shores of N and NW Spain. *Mar. Environ. Res.* **140**, 394–402 (2018).
47. Fernández, C. Current status and multidecadal biogeographical changes in rocky intertidal algal assemblages: the northern Spanish coast. *Estuar. Coast. Shelf Sci.* **171**, 35–40 (2016).
48. Eggert, A. Seaweed responses to temperature. In *Seaweed Biology. Novel Insights into Ecophysiology, Ecology and Utilization* (eds. Wiencke, C. & Bischof, K.) 47–66 (Springer, Berlin, 2012).
49. Karsten, U. Seaweed acclimation to salinity and desiccation stress. In *Seaweed biology. Novel Insights into Ecophysiology, Ecology and Utilization* (eds. Wiencke, C. & Bischof, K.) 87–108 (Springer, Berlin, 2012).
50. Phelps, C. M., Boyce, M. C. & Huggett, M. J. Future climate change scenarios differentially affect three abundant algal species in southwestern Australia. *Mar. Environ. Res.* **126**, 69–80 (2017).
51. Olabarria, C., Arenas, F., Fernández, Á., Troncoso, J. S. & Martínez, B. Physiological responses to variations in grazing and light conditions in native and invasive fucoids. *Mar. Environ. Res.* **139**, 151–161 (2018).
52. Schagerl, M. & Möstl, M. Drought stress, rain and recovery of the intertidal seaweed. *Fucus spiralis*. *Mar. Biol.* **158**, 2471–2479 (2011).
53. Lamela-Silvarrey, C., Fernández, C., Anadón, R. & Arrontes, J. Fucoid assemblages on the north coast of Spain: Past and present (1977–2007). *Bot. Mar.* **55**, 199–207 (2012).
54. Martínez, B., Arenas, F., Trilla, A., Viejo, R. M. & Carreño, F. Combining physiological threshold knowledge to species distribution models is key to improving forecasts of the future niche for macroalgae. *Glob. Change Biol.* **21**, 1422–1433 (2014).
55. Piñeiro-Corbeira, C., Barreiro, R., Cremades, J. & Arenas, F. Seaweed assemblages under a climate change scenario: Functional responses to temperature of eight intertidal seaweeds match recent abundance shifts. *Sci. Rep.* **8**, 1–9 (2018).
56. Figueroa, F. L. *et al.* Yield losses and electron transport rate as indicators of thermal stress in *Fucus serratus* (Ochrophyta). *Algal Res.* **41**, 101560 (2019).
57. Davison, I. R. & Pearson, G. A. Stress tolerance in intertidal seaweeds. *J. Phycol.* **32**, 197–211 (1996).
58. Schreiber, U., Bilger, W. & Neubauer, C. Chlorophyll Fluorescence as a Noninvasive Indicator for Rapid Assessment of In Vivo Photosynthesis. In *Ecophysiology of photosynthesis* (eds. Schulze, E.D. & Caldwell, M.M.) 49–70 (Springer, Berlin, 2003).
59. Hurd, K., Harrison, P.J., Bischof, K. & Lobban, C.S. Physico-chemical factors as environmental stressors in seaweed biology. In *Seaweed Ecology and Physiology* (eds. Hurd, K., Harrison, P.J., Bischof, K. & Lobban, C.S.) 294–348 (Cambridge University Press, Cambridge, 2014).
60. Kumar, M. *et al.* Desiccation induced oxidative stress and its biochemical responses in intertidal red alga *Gracilaria corticata* (Gracilariales, Rhodophyta). *Environ. Exp. Bot.* **72**, 194–201 (2011).
61. Bischof, K. & Rautenberger, R. Seaweed responses to environmental stress: Reactive oxygen and antioxidative strategies. In *Seaweed biology. Novel insights into Ecophysiology, Ecology and Utilization* (eds. Wiencke, C., Bischof, K.) 109–134 (Springer, Berlin, 2012).
62. Allakhverdiev, S. I. *et al.* Heat stress: An overview of molecular responses in photosynthesis. *Photosynth. Res.* **98**, 541–550 (2008).
63. Mota, C. F., Engelen, A. H., Serrão, E. A. & Pearson, G. A. Some don't like it hot: Microhabitat-dependent thermal and water stresses in a trailing edge population. *Funct. Ecol.* **29**, 640–649 (2015).
64. Hunt, L. J. H. & Denny, M. W. Desiccation protection and disruption: A trade-off for an intertidal marine alga. *J. Phycol.* **44**, 1164–1170 (2008).

65. Staehr, P. A. & Wernberg, T. Physiological responses of *Ecklonia radiata* (Laminariales) to a latitudinal gradient in ocean temperature. *J. Phycol.* **45**, 91–99 (2009).
66. Davison, I. R. & Davison, J. O. The effect of growth temperature on enzyme activities in the brown alga *Laminaria saccharina*. *Br. Phycol. J.* **22**, 77–87 (1987).
67. Young, E. B., Dring, M. J., Savidge, G., Birkett, D. A. & Berges, J. A. Seasonal variations in nitrate reductase activity and internal N pools in intertidal brown algae are correlated with ambient nitrate concentrations. *Plant, Cell Environ.* **30**, 764–774 (2007).
68. Monteiro, C. *et al.* Canopy microclimate modification in central and marginal populations of a marine macroalga. *Mar. Biodivers.* **49**, 415–424 (2019).
69. Dawes, C. J. Physiological ecology. In *Marine Botany* (ed. Dawes, C.J.) (Wiley, New York, 1998).
70. Rohde, S., Hiebenthal, C., Wahl, M., Karez, R. & Bischof, K. Decreased depth distribution of *Fucus vesiculosus* (Phaeophyceae) in the Western Baltic: Effects of light deficiency and epibionts on growth and photosynthesis. *Eur. J. Phycol.* **43**, 143–150 (2008).
71. Lüning, K. Seaweed vegetation of the cold and warm temperate regions of the northern hemisphere. In *Seaweeds. Their Environment, Biogeography and Ecophysiology*. (ed. Lüning, K.) (Wiley, New York, 1990).
72. Schiel, D. R., Lilley, S. A., South, P. M. & Coggins, J. H. J. Decadal changes in sea surface temperature, wave forces and intertidal structure in New Zealand. *Mar. Ecol. Prog. Ser.* **548**, 77–95 (2016).
73. Fernández de la Hoz, C. F. *et al.* OCLE: a European open access database on climate change effects on littoral and oceanic ecosystems. *Prog. Oceanogr.* **168**, 222–231 (2018).
74. Fernández de la Hoz, C., Ramos, E., Puente, A. & Juanes, J. A. Climate change induced range shifts in seaweeds distributions in Europe. *Mar. Environ. Res.* **148**, 1–11 (2019).
75. Crain, C. M., Kroeker, K. & Halpern, B. S. Interactive and cumulative effects of multiple human stressors in marine systems. *Ecol. Lett.* **11**, 1304–1315 (2008).
76. Halekoh, U., Hojsgaard, S. & Yan, J. The R package geepack for generalized estimating equations. *J. Stat. Softw.* **15**, 1–11 (2006).
77. Fox, J. *Applied Regression Analysis and Generalized Linear Models* 3rd edn. (Sage, Thousand Oaks, 2016).

Acknowledgements

This work was supported by the *Fundación Biodiversidad*, the Ministerio para la Transición Ecológica y el Reto Demográfico through the Pleamar program (2018 call), co-funded by the European Maritime and Fisheries Fund (EMFF). The authors thank Esther Pérez for valuable assistance and two reviewers for valuable suggestions in improving the manuscript.

Author contributions

C.O. and M.R. conceived the ideas and designed methodology. M.R., S.R., C.O., E.V. and J.T. collected the data. M.R., C.O. and S.R. analysed the data. M.R. and C.O. led the writing of the manuscript. All authors contributed critically to the drafts and gave final approval for publication.

Competing interests

The authors declare no competing interests.

Additional information

Supplementary information is available for this paper at <https://doi.org/10.1038/s41598-020-78526-5>.

Correspondence and requests for materials should be addressed to M.R.

Reprints and permissions information is available at www.nature.com/reprints.

Publisher's note Springer Nature remains neutral with regard to jurisdictional claims in published maps and institutional affiliations.



Open Access This article is licensed under a Creative Commons Attribution 4.0 International License, which permits use, sharing, adaptation, distribution and reproduction in any medium or format, as long as you give appropriate credit to the original author(s) and the source, provide a link to the Creative Commons licence, and indicate if changes were made. The images or other third party material in this article are included in the article's Creative Commons licence, unless indicated otherwise in a credit line to the material. If material is not included in the article's Creative Commons licence and your intended use is not permitted by statutory regulation or exceeds the permitted use, you will need to obtain permission directly from the copyright holder. To view a copy of this licence, visit <http://creativecommons.org/licenses/by/4.0/>.

© The Author(s) 2020